Supporting Information

Correlating Orbital Overlap Area and Vibrational Frequency Shift of Isocyanide Moiety Adsorbed on Pt and Pd Covered Au(111) Surfaces

Xia-Guang Zhang*[a], Jin-Hui Zhong*[b]

[a] Key Laboratory of Green Chemical Media and Reactions, Ministry of Education, Collaborative Innovation Center of Henan Province for Green Manufacturing of Fine Chemicals, College of Chemistry and Chemical Engineering, Henan Normal University, Xinxiang 453007, China

[b] Department of Materials Science and Engineering, Southern University of Science and Technology, Shenzhen, 518055, China

*Email: zhangxiaguang@htu.edu.cn, zhongjh@sustech.edu.cn

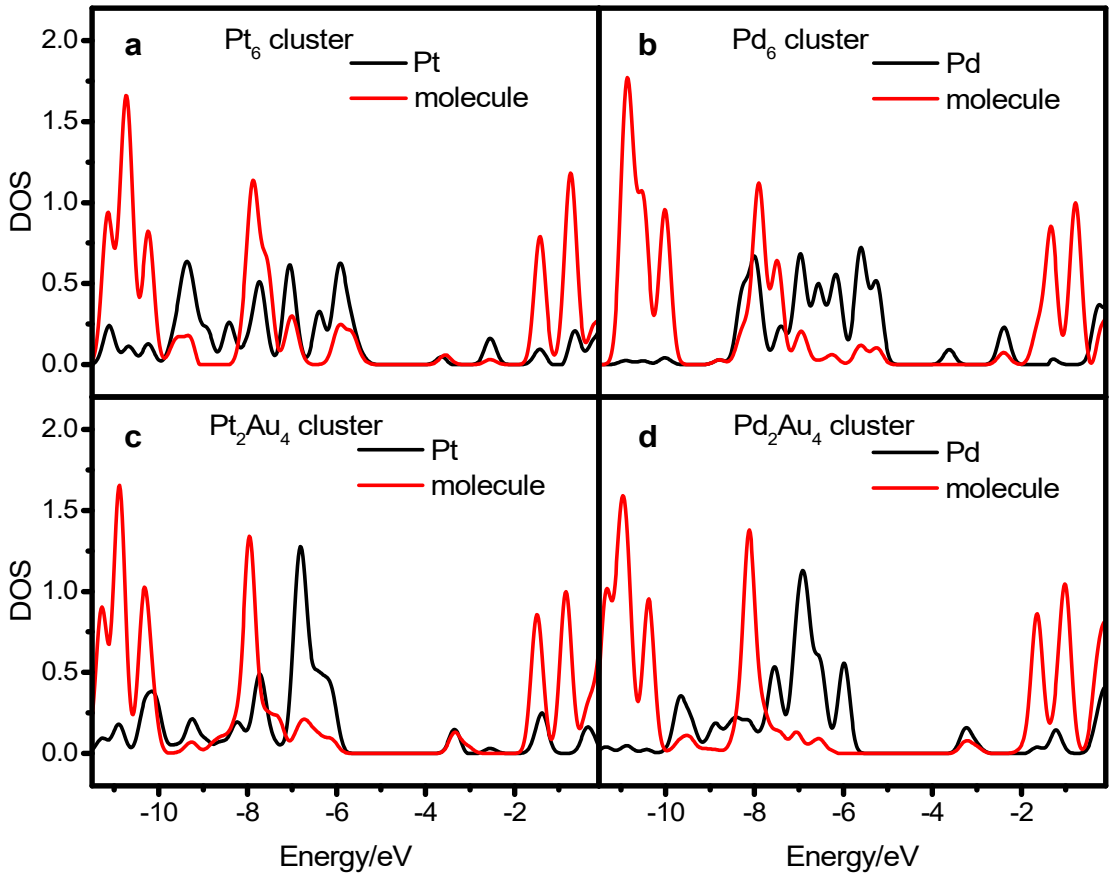

Fig. S1 Density of states (DOS) of PIC molecule adsorption on the top site of (a) Pt_6, (b) Pd_6, (c) Pt_2Au_4, and (d) Pd_2Au_4 clusters. The black and red line represent the DOS of absorbed Pt/Pd atom, and PIC molecule, respectively.

Fig. S1 shows the DOS of PIC adsorption on top site of four different clusters. Although a strong bonding interaction of metal atom and PIC can be found, the large overlap of unoccupied orbital (antibonding) is also apparent. The band gap of Pt_6 and Pd_6 clusters are smaller than that of Pd_2Au_4 and Pd_2Au_4 clusters, suggesting that the pure Pt and Pd clusters can form antibonding interaction with C≡N more easily than Pt and Pd alloyed with Au, respectively. This may be the main reason of the smaller $\upsilon_{C\equiv N}$ frequency shift for PIC adsorbed on pure Pt and Pd clusters compared to the respective alloy ones.

Table S1. Main orbitals of extended charge decomposition analysis for PIC adsorption on Pd_6, Pt_6, Pd_2Au_4, Pt_2Au_4 clusters based on PBE1PBE functional. The d, b, and r represent charge transfer from metal to PIC, PIC to metal, and charge polarization, respectively.

cluster	orbital	d	b	r
Pd_6	80	0.003943	0.096214	-0.227154
	76	0.029549	-0.000503	-0.040383
	74	0.024007	-0.000955	-0.027486
	71	0.015707	0.009200	-0.063112
	65	0.202452	-0.046360	0.029389
	58	-0.034232	-0.070371	0.007202
	56	-0.019701	-0.027769	-0.001632
	51	0.011471	0.000379	0.016543
	50	-0.047084	-0.047936	-0.002819
	45	-0.086376	0.180354	0.196562
	42	-0.014286	0.004968	0.007264
	40	-0.027440	0.002410	-0.000481
	37	-0.001879	0.010324	0.003384
	33	-0.001212	-0.055255	-0.003178
Pt_6	78	-0.086811	0.004648	-0.571108
	75	0.043878	-0.001520	-0.075504
	74	0.040739	-0.002197	-0.051272
	69	-0.006733	-0.289978	-0.373341
	57	-0.254817	-0.016644	-0.009620
	55	-0.751941	-0.550892	-0.842085
	48	-0.034597	-0.021414	-0.023793
	47	-0.579313	-0.471612	-0.554431
	41	-0.112284	-0.294001	-0.026536
	40	-0.021504	-0.099551	0.002551
	15	-0.023190	-0.023348	-0.090552
Pd_2Au_4	83	-0.072519	0.019661	-0.024125
	78	0.015701	0.000053	-0.020685
	77	-0.066243	0.017338	-0.011750
	76	0.012470	0.001047	-0.033093
	75	0.010593	0.002139	-0.033185
	71	0.019772	0.000438	-0.023211
	68	-0.019793	-0.008728	-0.041976
	65	0.011943	-0.003246	-0.007492
	61	0.038536	-0.001743	-0.000483
	59	-0.117145	-0.009934	-0.010782
	58	-0.048397	-0.004395	0.001737
	56	-0.095475	-0.042110	-0.007333

	54	-0.007077	-0.048160	-0.004946
	53	-0.015429	-0.012450	-0.004433
	52	-0.015419	0.004801	0.001123
	50	0.099956	-0.007472	-0.009822
	49	0.012861	-0.007161	0.029265
	43	-0.133506	0.102742	0.119383
	42	-0.117370	0.050122	0.069771
	40	-0.036027	0.007556	0.002953
	33	-0.000237	-0.018752	-0.000834
	27	-0.016844	-0.010155	0.042349
	13	0.012574	-0.001272	0.016059
Pt_2Au_4	83	0.014999	-0.001265	-0.031751
	82	0.016627	-0.000889	-0.006666
	81	0.015965	-0.002688	0.003047
	80	0.018068	-0.011410	0.000928
	79	0.013005	0.000003	-0.027809
	78	0.010742	-0.001381	-0.049019
	77	0.039324	-0.004447	-0.035554
	75	-0.682798	-0.727869	-1.454780
	74	-0.014623	0.002432	-0.003582
	73	0.035463	0.000171	-0.081389
	70	-0.017372	-0.004159	-0.007083
	68	-0.061412	-0.051771	-0.073997
	67	-0.326870	-0.172237	-0.278385
	66	0.011626	0.000058	0.019531
	64	-0.007787	-0.091934	-0.085901
	62	-0.021156	-0.027896	-0.035923
	61	-0.064526	-0.113166	-0.153268
	59	-0.011546	-0.010298	-0.026405
	57	-0.048142	-0.067412	-0.082907
	54	-0.071117	-0.002601	-0.007256
	53	-0.611753	-0.406705	-0.612022
	50	-0.230687	-0.166030	-0.230650
	47	-0.239581	-0.172734	-0.196062
	46	-0.012550	-0.010589	0.044722
	41	-0.125193	-0.181780	-0.181151
	40	-0.030253	-0.077972	-0.055462
	39	-0.010567	-0.019225	-0.016400
	33	-0.004333	-0.037287	-0.011699
	27	-0.031388	-0.026330	-0.102783
	13	0.022430	-0.003913	0.030087

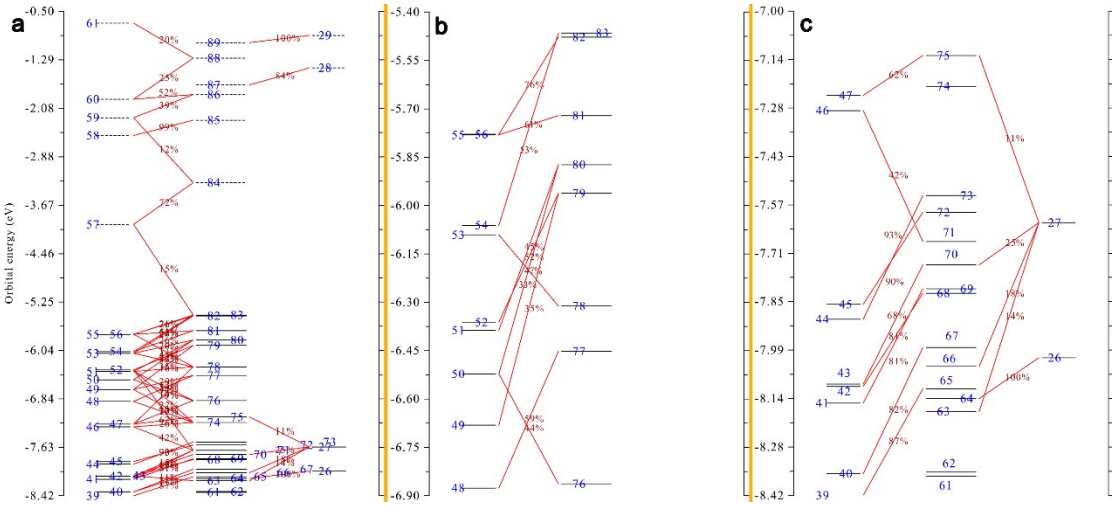

Fig. S2 Orbital interaction diagram of PIC adsorption on Pd_2Au_4 cluster, three columns are the orbital of Pd_2Au_4 fragment, complex of PIC-Pd_2Au_4, and PIC molecule, respectively. (b) and (c) are the zoom-in of the energy region of (a) from -6.90 to -5.40 eV and -8.42 to -7.00 eV, respectively, and the contribution from Pd_2Au_4 fragment to complex is set to 30%.

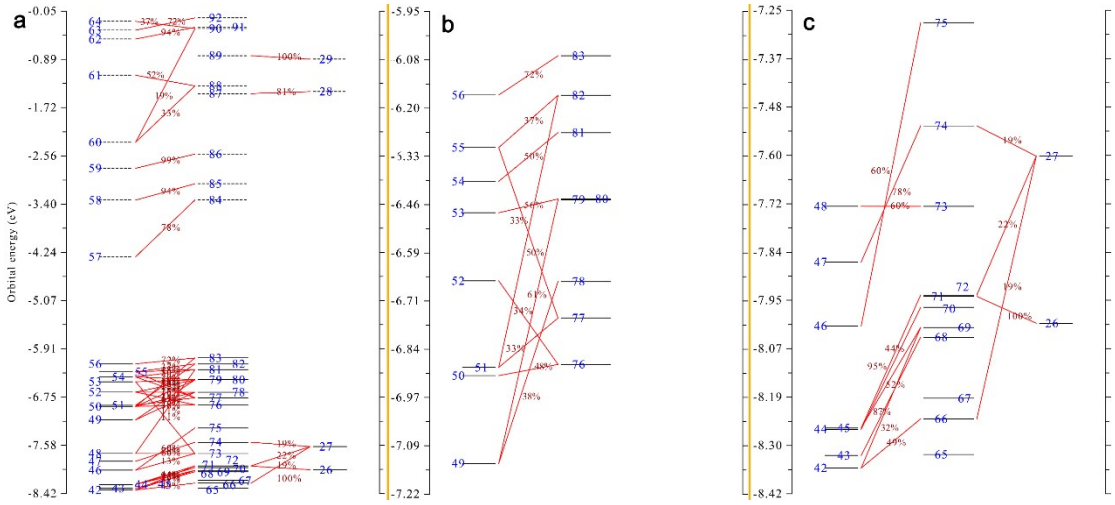

Fig. S3 Orbital interaction diagram of PIC adsorption on Pt_2Au_4 cluster, three columns are the orbital of Pt_2Au_4 fragment, complex of PIC-Pt_2Au_4, and PIC molecule, respectively. (b) and (c) are the zoom-in of the energy region of (a) from -7.22 to -5.95 eV and -8.42 to -7.25 eV, respectively, and the contribution from Pt_2Au_4 fragment to complex is set to 30%.

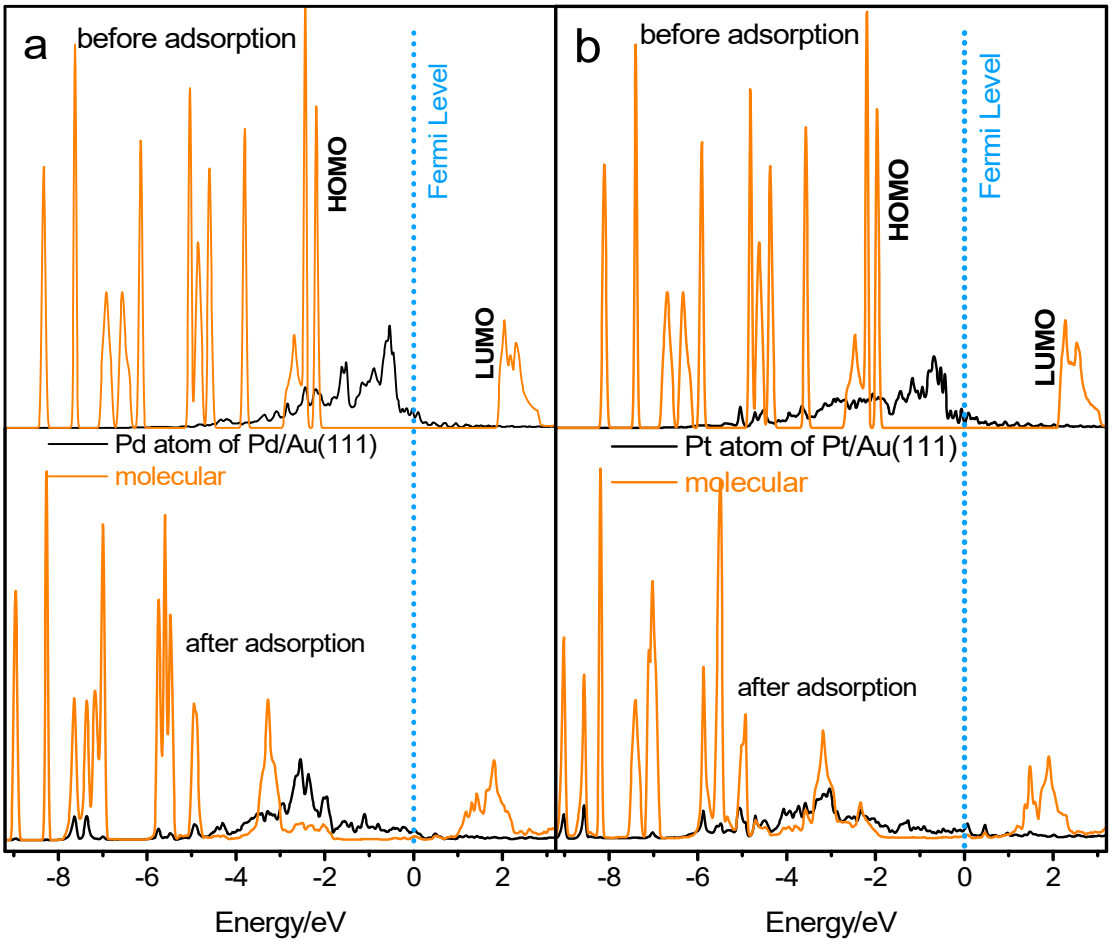

Fig. S4 Orbital interaction diagram of PIC before and after adsorption on top site of mono-layer Pd/Au(111) (a) and Pt/Au(111) (b) surface, the black and orange lines are *d* orbital Pd (Pt) atom and orbital molecular of PIC, respectively. The energy is referred to the Fermi energy level.

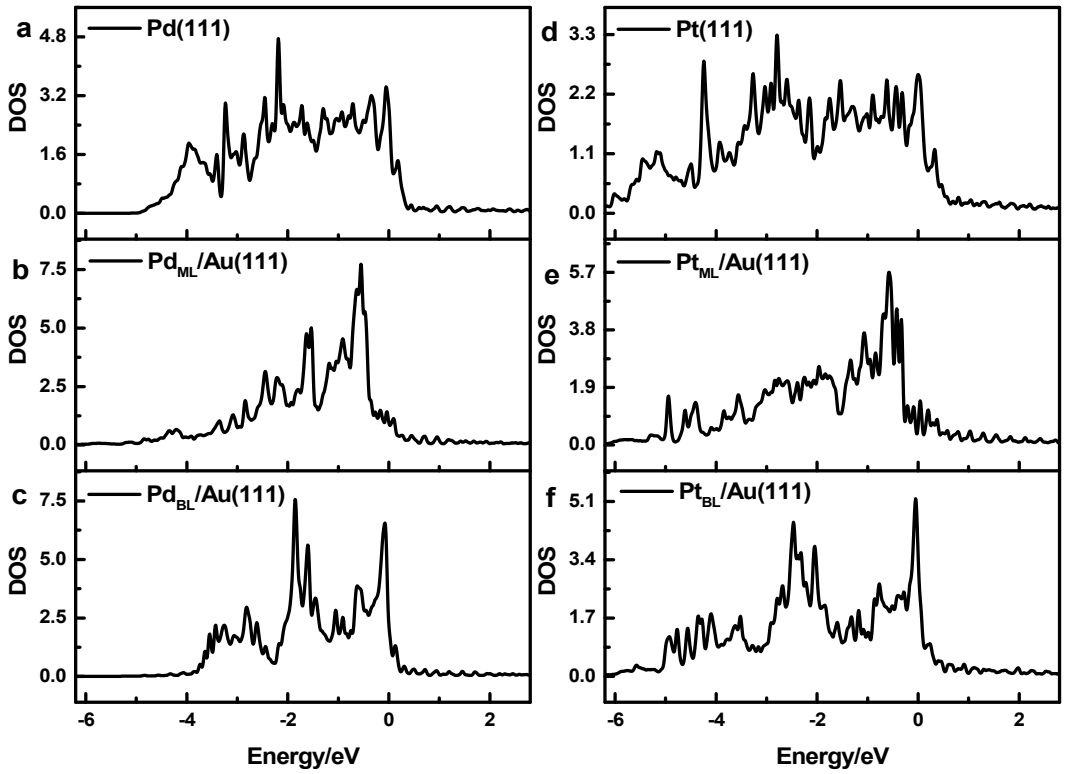

Fig. S5 *d*-electrons DOS of surface atoms of (a) clean Pd(111), (b) Pd_{ML}/Au(111), (c) Pd_{BL}/Au(111), (d) Pt(111), (e) Pt_{ML}/Au(111), and (f) Pt_{BL}/Au(111).

Table S2. Bond lengths (Å) of C-Pd(Pt) for PIC adsorbed on the top site of Pt/Au(111) and Pt/Au(111) surfaces.

	PIC		Cl-PIC		NH_2-PIC		CF_3-PIC	
	Pd	Pt	Pd	Pt	Pd	Pt	Pd	Pt
Mono-layer	1.883	1.860	1.881	1.859	1.885	1.862	1.879	1.858
Bi-layer	1.878	1.857	1.878	1.857	1.882	1.860	1.876	1.855

Table S3. N≡C-Ph bond angle (degree) of PIC adsorbed on the top site of Pt/Au(111) and Pt/Au(111) surfaces.

	PIC		Cl-PIC		NH_2-PIC		CF_3-PIC	
	Pd	Pt	Pd	Pt	Pd	Pt	Pd	Pt
Mono-layer	179.9	178.8	179.9	179.8	178.9	178.6	179.4	178.6
Bi-layer	179.5	178. 8	179.7	179.4	179.3	178.6	179.3	179.0
Free	180.0		179.9		179.2		179.3	

Table S4. C≡N bond lengths (Å) of PIC and its derivatives adsorbed on the top site of Pt/Au(111) and Pt/Au(111) surfaces.

	PIC		Cl-PIC		NH_2-PIC		CF_3-PIC	
	Pd	Pt	Pd	Pt	Pd	Pt	Pd	Pt
ML	1.187	1.184	1.188	1.185	1.187	1.184	1.189	1.186
BL	1.188	1.185	1.189	1.186	1.187	1.184	1.189	1.187
Free	1.900		1.186		1.185		1.186	

Table S5. NC-Ph bond lengths (Å) of PIC adsorbed on the top site of Pt/Au(111) and Pt/Au(111) surfaces.

	PIC		Cl-PIC		NH_2-PIC		CF_3-PIC	
	Pd	Pt	Pd	Pt	Pd	Pt	Pd	Pt
ML	1.372	1.371	1.369	1.369	1.370	1.370	1.369	1.369
BL	1.372	1.370	1.370	1.368	1.371	1.368	1.370	1.367
Free	1.378		1.379		1.378		1.379	

Table S6. Bonding energies (Ry) of molecular adsorption on Pd/Au(111) and Pt/Au(111) surfaces.

	PIC		Cl-PIC		NH_2-PIC		CF_3-PIC		HCN		CO	
	Pd	Pt	Pd	Pt	Pd	Pt	Pd	Pt	Pd	Pt	Pd	Pt
ML	-0.169	-0.184	-0.121	-0.135	-0.121	-0.136	-0.120	-0.134	-0.123	-0.144	-0.108	-0.122
BL	-0.178	-0.208	-0.129	-0.159	-0.128	-0.160	-0.128	-0.158	-0.131	-0.170	-0.116	-0.148

Table S7. Calculated *d*-band center in eV for the Pd_{ML}/Au(111), Pd_{BL}/Au(111), Pt_{ML}/Au(111), Pt_{BL}/Au(111), Pd(111), and Pt(111) surfaces.

Pd_{ML}/Au(111)	Pd_{BL}/Au(111)	Pt_{ML}/Au(111)	Pt_{BL}/Au(111)	Pd(111)	Pt(111)
-1.405	-1.386	-1.646	-1.852	-1.677	-2.127

Table S8. $\upsilon_{C\equiv N}$ frequency (cm^{-1}) of molecules with and without adsorption on the top site of Pd/Au(111) and Pt/Au(111) surfaces.

	PIC		Cl-PIC		NH_2-PIC		CF_3-PIC		HCN		CO	
	Pd	Pt	Pd	Pt	Pd	Pt	Pd	Pt	Pd	Pt	Pd	Pt
ML	2122	2179	2129	2175	2132	2178	2125	2164	1991	2021	2045	2073
BL	2129	2170	2122	2157	2128	2171	2122	2159	1992	2011	2044	2050
free	2118		2119		2115		2119		2017		2147	

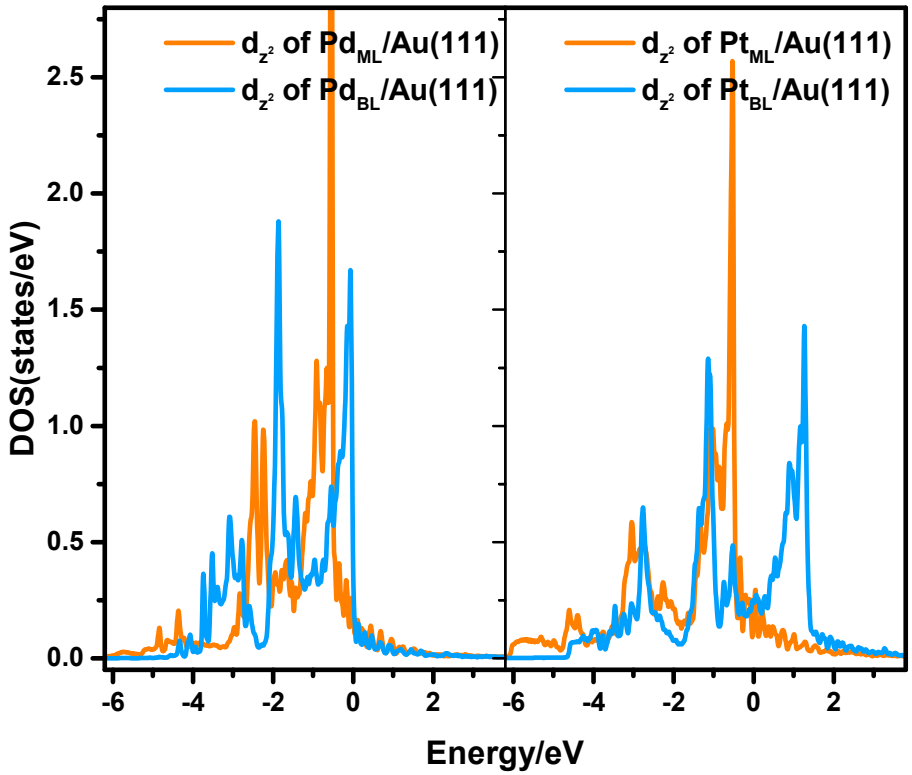

Fig. S6 d_{z2}-electrons project DOS of surface Pd and Pt atom for (a) Pd/Au(111) and (b) Pt/Au(111) surfaces.

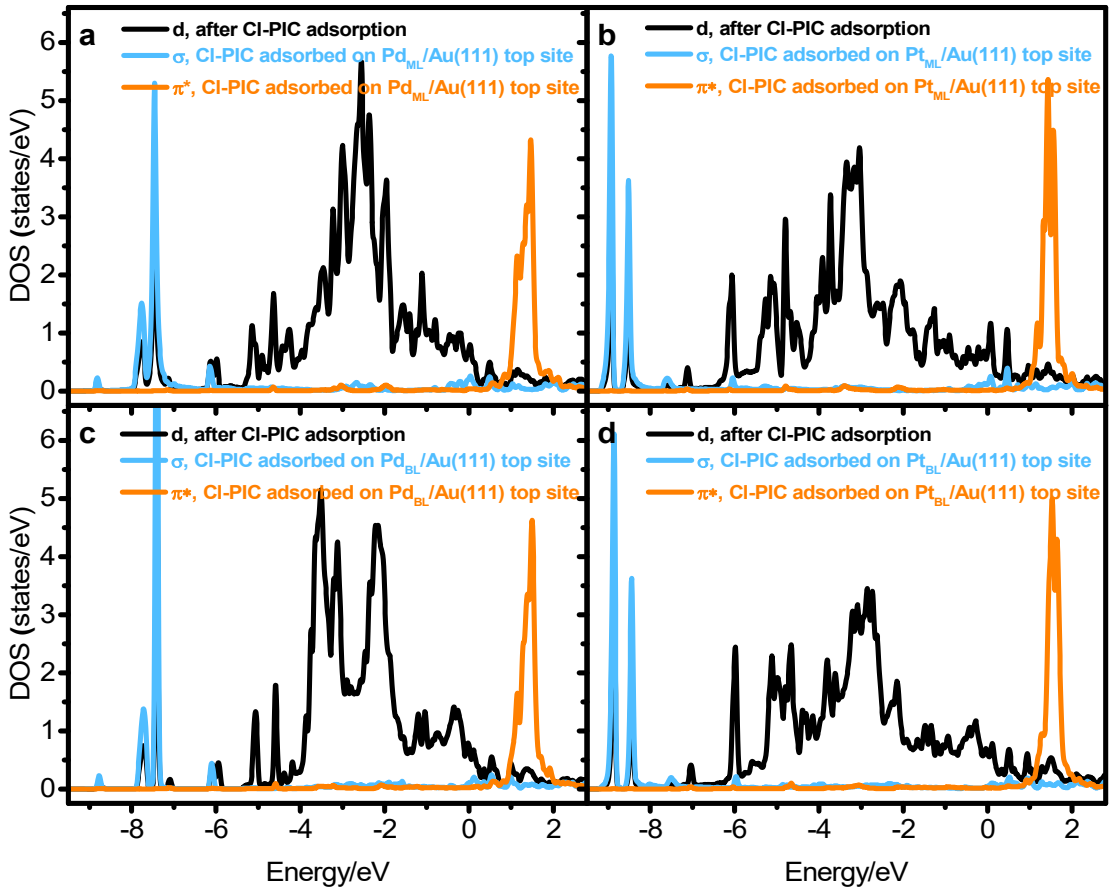

Fig. S7 DOS of Cl-PIC adsorption on the top site of (a) Pd_{ML}/Au(111), (b) Pt_{ML}/Au(111), (c) Pd_{BL}/Au(111), and (d) Pt_{BL}/Au(111) surfaces. The energy is relative to the Fermi level, and black, red, and orange lines represent the DOS of *d* orbital of adsorbed metal atom, σ orbital and π^* orbital of adsorbed Cl-PIC, respectively.

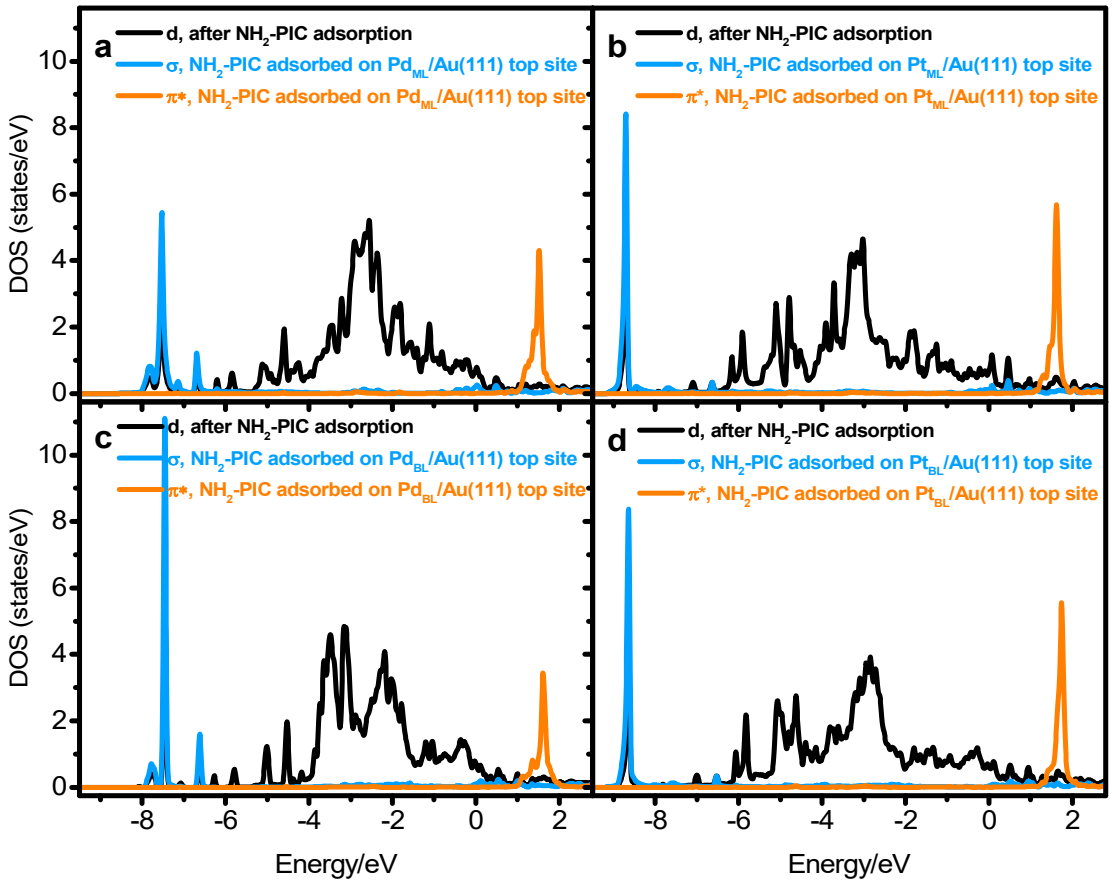

Fig. S8 DOS of NH_2-PIC adsorption on the top site of (a) Pd_{ML}/Au(111), (b) Pt_{ML}/Au(111), (c) Pd_{BL}/Au(111), and (d) Pt_{BL}/Au(111) surfaces. The energy is relative to the Fermi level, and black, red, and orange lines represent the DOS of *d* orbital of adsorbed metal atom, σ orbital and π^* orbital of adsorbed NH_2-PIC, respectively.

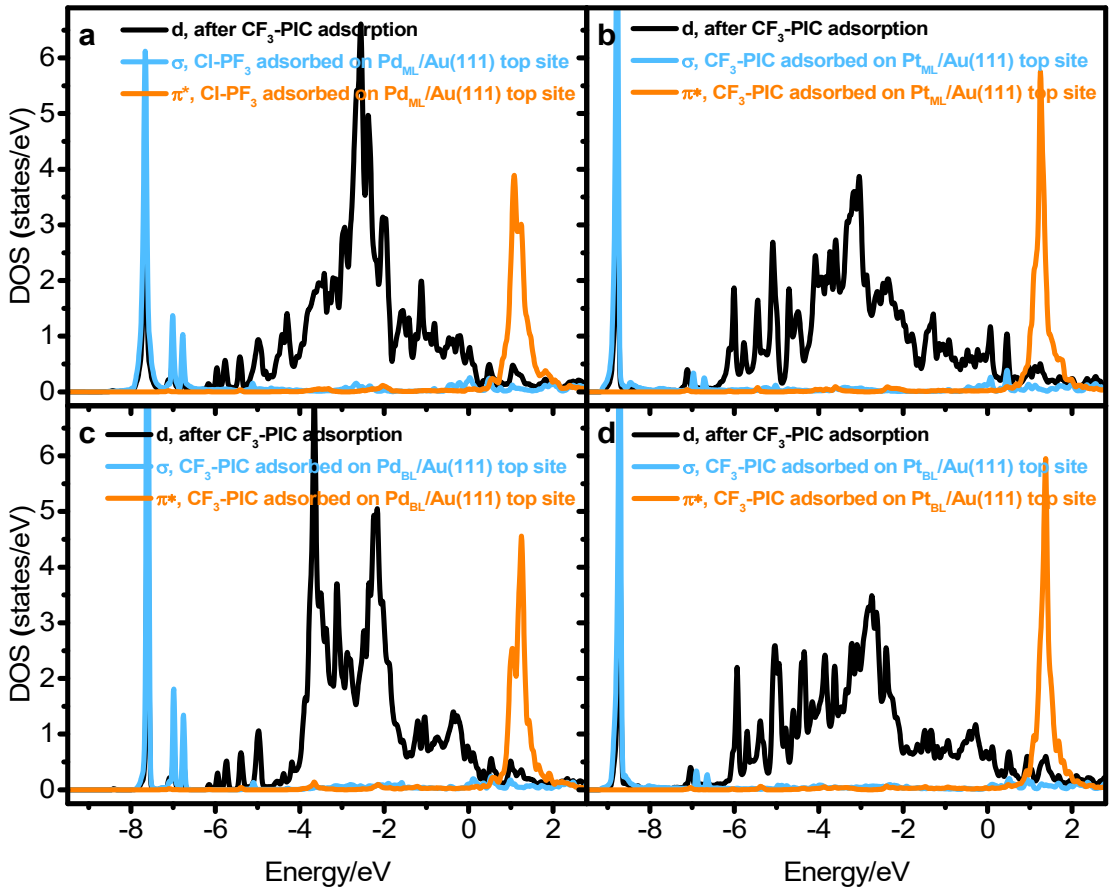

Fig. S9 DOS of CF_3-PIC adsorption on the top site of (a) Pd_{ML}/Au(111), (b) Pt_{ML}/Au(111), (c) Pd_{BL}/Au(111), and (d) Pt_{BL}/Au(111) surfaces. The energy is relative to the Fermi level, and black, red, and orange lines represent the DOS of *d* orbital of adsorbed metal atom, σ orbital and π^* orbital of adsorbed CO, respectively.

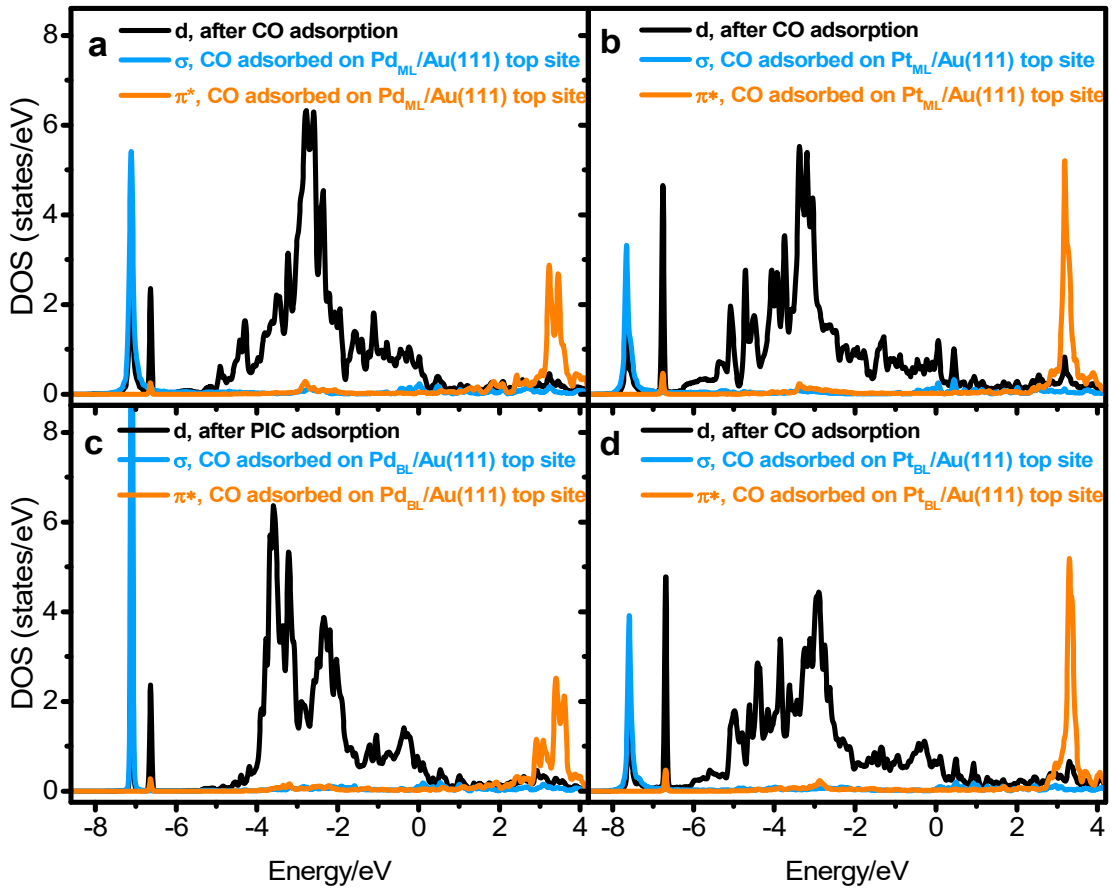

Fig. S10 DOS of CO adsorption on the top site of (a) Pd_{ML}/Au(111), (b) Pt_{ML}/Au(111), (c) Pd_{BL}/Au(111), and (d) Pt_{BL}/Au(111) surfaces. The energy is relative to the Fermi level, and black, red, and orange lines represent the DOS of *d* orbital of adsorbed metal atom, σ orbital and π* orbital of adsorbed CO, respectively.